Assessment of ultrasound assisted coalescence of water-in-crude oil emulsion: Influence of piezoelectric transducer material under batch and continuous conditions

Idowu Adeyemi [1], Mahmoud Meribout[b], Lyes Khezzar[c], Nabil Kharoua[c], Khalid AlHammadi[b]

[a]Department of Mechanical Engineering, Khalifa University of Science and Technology, P.O. Box 127788, Abu Dhabi, United Arab Emirates
[b]Department of Electrical Engineering and Computer Science, Khalifa University of Science and Technology, P.O. Box 127788, Abu Dhabi, United Arab Emirates
[c]Department of Mechanical Engineering, Ecole Nationale Polytechnique de Constantine, Constantine, Algeria

Abstract

In this work, the potentiality of lead free ultrasound (US) materials towards crude oil emulsion demulsification was assessed. The assessment is crucial because of the detrimental environmental and health impacts of lead zirconate titanate, which is widely used for US coalescence presently. The production or utilization of lead zirconate titanate (PZT) results in the release of vaporized hazardous lead oxide (PbO) at elevated temperature or dissolution of poisonous lead into aqueous medium. Hence, the analysis of the effect of different piezoelectric material type (PZT, polyvinylidene fluoride (PVDF) and lithium niobate ($LiNbO_3$)) on domain acoustic pressure distribution and the subsequent coalescence of binary droplets under batch conditions was conducted. The lead-free piezoelectric materials (PVDF and $LiNbO_3$) were assessed with the PZT in order to determine their viability for droplet coalescence. The piezoelectric materials were subjected to mechanical oscillation under resonance in order to allow for optimum performance. Moreover, the US coalescence was examined under continuous flow conditions to determine coalescence behavior and performance during online emulsion treatment. The eigen-frequency analysis provided the resonance frequencies of 19.61, 26.04 and 57.80 kHz for PVDF, PZT and Lithium niobate, respectively. Moreover, the acoustic pressure in the emulsion domain varied in magnitude and distribution. The order of the coalescence time for the binary droplets followed the order PZT<PVDF<$LiNbO_3$. Furthermore, increasing the flow velocities resulted in slight reduction in the coalescence time and energy consumed for the different piezoelectric materials evaluated.

1. Introduction

Due to the health and environmental concerns associated with the utilization of lead zirconate titanate (PZT), there has been stringent regulatory attempts to limit or stop their usage [1-3]. PZT poses major health challenges during production and usage due to the vaporization of lead oxide at elevated temperature, addition of unique dopants, and zirconate to titanate ratio [3, 4]. Although the vaporized lead oxide (median lethal dose of 4.3g/kg) in PZT ceramics have lower toxicity as compared to lead (median lethal dose of 0.45g/kg), the hazard caused due to the vaporization of lead oxide is complicated due to their

elevated vapor pressure. Moreover, there is a report that showed that PZT ceramics could have unstable conditions in water, with the lead dissolving in aqueous media [5]. The dissolution of lead in aqueous media raises further concerns as the lead content in these transducers could reach up to 60wt% [6]. Hence, regulatory bodies have enacted limitations on the usage of lead and lead containing substances. For instance, the European Union (EU) in 2012 included PZT amongst substances of very high concern (SVHC) in the REACH regulation [7-8].

The strict regulation of the usage of lead in piezoelectric materials has resulted in increased attention for lead free piezoelectric materials. The evaluated lead-free piezoelectric materials have been studied for their utilization in actuators,

Corresponding author. Tel.: +97123124338
Fax: +97123124338; E-mail: idowu.adeyemi@ku.ac.ae

sensor and transducers. Different materials such as barium titanate, potassium sodium niobate, lithium niobate, Rochelle salt, polyvinylidene fluoride (PVDF), quartz have shown promising results [3, 9-13]. For instance, lithium niobate provided enhanced performance over PZT under increased frequency and temperature applications. PZTs possess less Curie temperature and mechanical quality factor [14]. In addition, polyvinylidene fluoride (PVDF) has been reported to have better impedance and flexibility over PZTs [15]. However, the replacement of PZT remains challenging despite the progress in the development of lead-free piezoelectric materials. The key issues arise due to the stability and relatively high piezoelectric coefficient (up to 600 pC/N d33 piezoelectric coefficients) of PZTs as well as the cost and availability of the lead-free substitutes [3].

PZTs continue to be the dominant piezoelectric material in most ultrasonic transducer applications including dewatering of water in oil emulsion, membrane desalination, clinical studies etc. These transducers have been examined for their usage in droplet coalescence and demulsification of water-in-oil emulsions due to the drawbacks of the persistence of emulsions in crude oil processes. Emulsions could lead to poising of refinery catalyst, elevation of cost of pumping them, blockage and wearing of parts. In one study, Luo et al [16] studied the coalescence of two water droplets in white oil under ultrasonic standing waves. A frequency of 20kHz was used for the PZT in a rectangular cell ($0.63 \times 0.92 \text{cm}^2$) at 20C. They observed that maximum coalescence was achieved at an intensity of 4.88W/cm^2. In another study, Xu [17] examined the numerical model of the coalescence of two air bubbles in water at 20kHz. They reported that at elevated acoustic pressure, the bubbles were compressed and aggregated at the antinode. These studies are focused on the usage of PZT transducers.

Although lead free transducers have been designed, they are very few and their application in droplet coalescence and dehydration of water-in-oil emulsions is very rare. Therefore, there is a significant need for the increased assessment of these lead-free piezoelectric materials towards droplet coalescence. Hence, in this study, the analysis of the effect of different piezoelectric material type (PZT, PVDF and LiNbO₃) on domain acoustic pressure distribution and the subsequent coalescence of binary droplets under batch and continuous mode was conducted. The lead-free piezoelectric materials (PVDF and LiNbO₃) were assessed with the PZT in order to determine their viability. The piezoelectric materials were subjected to mechanical oscillation under resonance in order to allow for optimum performance.

2. Numerical Methods

2.1. Model Description and Boundary Conditions

The numerical model was developed for the assessment of the effect of piezoelectric material type (PZT, PVDF and Lithium niobate) on the acoustic pressure and coalescence time under batch and continuous flow conditions. The numerical analysis was conducted with COMSOL Multiphysics 5.6, and consists of the solid mechanics, electrostatic, pressure acoustic, laminar flow and phase field models. The transducers were actuated based on the resonance frequencies of each material. The model is based on phase field ultrasound assisted interfacial gravitational settling of water droplets in continuous oil emulsion. It consists of a 2 inches rectangular central plane of a

cylindrical pipe of diameter of 2 inches (Fig. 1a). The boundary of the plane consists of two walls along the width. The inlet and outlet, which were implemented with varying flow conditions, are on the planar heights on the two sides. The fluid consists of two water droplets in crude oil emulsion. The geometry mesh consists of 58.9k, 101.5k and 663k mesh elements for the PVDF, PZT and LiNbO₃, respectively (Fig. 1b). The mesh elements satisfy the minimum mesh requirements for acoustic propagation based on h<c/f/5. Where h is the minimum element size, c is speed of sound and f is the resonance frequencies for the different materials.
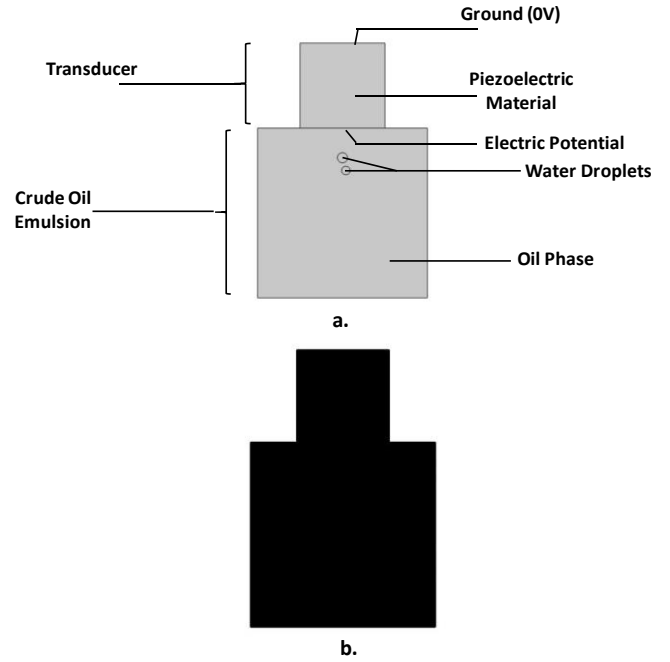
Fig. 1. a. Set-up of the ultrasound droplet coalescence **b.** Geometry Mesh

2.2. Governing Equations

The finite element model of the ultrasound assisted gravitational settling and coalescence of two water droplets in continuous oil emulsion was developed with COMSOL. The domain is governed by the wave equation:

$$\nabla \cdot \left(-\frac{1}{\rho}(\nabla p_t - q_d) \right) - \frac{k_{eq}^2 p_t}{\rho} = Q_m \tag{1}$$

Where $p_t = p + p_b$ and $k_{eq}^2 = \left(\frac{\omega}{c}\right)^2 - k_z^2$

Where ρ is the piezoelectric domain density, pt is the total pressure, pb is the background pressure, qd is the monopole domain source, keq is the wave number consisting of the ordinary wave number k, the azimuthal wave number and the out of plane wave number kz, Qm is the monopole domain source, and c is the speed of sound

In addition, the model consists of fluid flow governing equations such as the continuity equation, Navier-Stokes momentum conservation equation and the level set functions. In order to ensure that the mass of the system is conserved, the following continuity equation was used [18]:

$$\nabla \cdot u = 0 \tag{2}$$

Where u is the velocity of the fluid and ∇ is the del operator

The conservation of momentum is as shown in equation 2 [18, 21-23]. It was included through the Navier-Stokes equation which is based on the Newton second law of motion. The momentum conservation comprises of the forces due to pressure gradient, diffusive-viscous forces, gravitational forces and interfacial force between the water and oil layers on the right hand side. The acceleration terms include the convective and transient components on the left hand side.

$$\rho \frac{\partial u}{\partial t} + \rho(u.\nabla)u = -\nabla p + \left(\mu(\nabla u + \nabla u^T)\right) + F_\sigma + F_{ac} + \rho g$$

(3)

Where u is the velocity of the fluid, t is the time, ρ is the density, μ is the viscosity, g is the gravitational force, F_γ is the interfacial tension and Fac is the acoustic force.

The interfacial force is represented as [21-22]:

$$F_\gamma = \nabla \cdot \left(\gamma(I - (nn^T))\delta\right)$$

(4)

Where γ is the coefficient of surface tension, δ is the Dirac function's smooth approximation, n is the normal at the interface and I is an identity matrix. The Dirac function approximation and the normal are functions of the level set functions of the interface

The density and viscosity are described as follows [18]:

$$\rho = \rho_w + (\rho_o - \rho_w)\phi$$

(5)

$$\mu = \mu_w + (\mu_o - \mu_w)\phi$$

(6)

Where ρ_w is the water density, ρ_o is the oil density, μ_w is the water viscosity, μ_o is the oil viscosity, ϕ is the level set smooth set function.

The interface layers were modeled with the level set multiphase flow equation as follows [19-20]:

$$\frac{\partial \phi}{\partial t} + u \cdot \nabla \phi = \gamma \nabla \cdot \left(\epsilon \nabla \phi - \phi(1-\phi)\frac{\nabla \phi}{|\nabla \phi|}\right)$$

(7)

Where ϕ is the level set smooth set function, u is the velocity of the fluid, t is the time, γ is the re-initialization parameter for numerical stability, ϵ is associated with interface thickness and represents half of the peak mesh element size

The no flow condition was specified at the boundaries to ensure there was no inflow and outflow of fluids in the system. The no flow condition was implemented as follows [18]:

$$n \cdot \left(\epsilon \nabla \phi - \phi(1-\phi)\frac{\nabla \phi}{|\nabla \phi|}\right) = 0$$

(8)

Where ϕ is the level set smooth set function, and n is the normal at the boundary. Moreover, no slip condition with zero velocity and wetted wall to account for the wall interface was implement taking the contact angle of the oil and water with the wall into consideration

The resonance frequency was determined through the eigen-frequency analysis. The following eigen-value equation was considered:

$$-\omega^2 + 2i\zeta\omega_0\omega + \omega_0^2 = 0$$

(9)

$$\text{Where} \quad \omega_0 = \sqrt{\frac{k}{m}} \quad \text{and} \quad \zeta = \frac{c}{2\sqrt{km}}$$

(10)

$$u = \tilde{u}e^{-\zeta\omega_0 t}e^{i\sqrt{1-\zeta^2}\omega_0 t}$$

(11)

Where ω is the resonance and higher angular frequencies, k is the stiffness constant, m is the mass, c is the damping coefficient, u is the displacement, t is time and ζ is the damping ratio.

3. RESULTS AND DISCUSSIONS

3.1. Model Validation

The droplet coalescence time in this study was validated with the experimental data of Luo et al [16] (Fig. 2). The validation was assessed at three binary droplet diameter pairs (275, 400 and 550 micrometers) at a frequency of 40 kHz. There was a reasonable agreement between the developed model and the experimental data in terms of the magnitude at each diameter and the trend with increasing diameter. Hence, the numerical model was utilized for the evaluation of different piezoelectric materials.
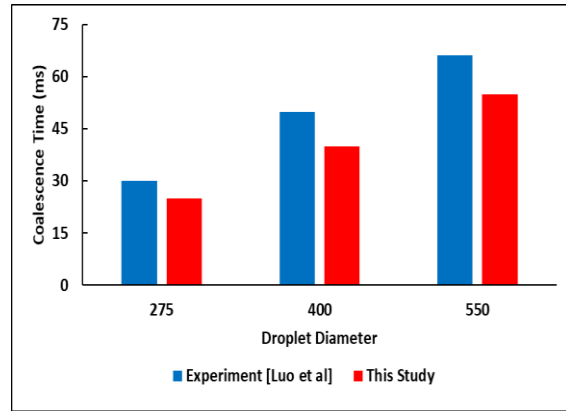
Fig. 2. Numerical model validation

3.2. Eigenvalue Analysis

The resonant frequencies of the three piezoelectric materials (PZT, PVDF and Lithium Niobate) were determined based on the eigenfrequency analysis. The resonance frequency estimation allows for the optimum actuation of the piezoelectric materials as they have different values. The natural frequencies are 19.61, 26.04 and 57.80 kHz for PVDF, PZT and Lithium niobate, respectively. Similar observation of the resonance frequency for PZT has been reported by other studies [24-27]. For instance, Tsujino et al [24] assessed the vibration and resonance frequency of a transducer consisting of four PZT disks with a thickness of 0.5cm and diameter of 4 cm. They reported a natural frequency of 26.70 kHz and a vibration of 1.44 times that of 40 kHz. In another study, similar result was found by Tsujino et al [25] with a natural frequency of 26.09 kHz reported for PZT. Other studies include the work of Nakamura et al [26] where they determined the natural frequency to be 28 kHz for a push-pull multi layered PZT actuator. Bawiec et al [27] stated that for PZT of radius 0.6-1cm and thickness 0.05cm, a resonance frequency was determined.

Based on the determined natural frequencies for the piezoelectric materials, the displacement of the transducer was determined. The displacement of the piezoelectric materials ranges from 0-18.3x10^{-7}, 0-14.0x10^{-7} and 0-14x10^{-7}m for Lithium niobate, PZT and PVDF, respectively (Fig. 3). The main

vibration mode for Lithium niobate is flextural, while the main vibration mode for PZT and PVDF are linear (compression and expansion). These types of vibration are common for piezoelectric actuation with frequencies lower than 100kHz. In their work, Panda and Sahoo [28] reported a displacement measurement of $10-12 \times 10^{-6}$m for PZT multilayer stack based on a dial gauge experiment. The PZT was a rectangular stack and has a different area ($1.32cm^2$) compared to the area of the PZT ($5.067cm^2$) utilized in this study. In addition, considering that this study is a 2D numerical model, the experimental data of Panda and Sahoo [28] provides a reasonable indication of the reliability of the COMSOL predictions of the displacement.
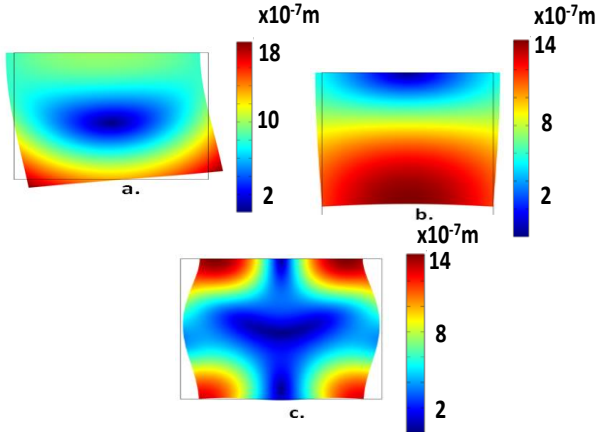
Fig. 3. Displacement of the piezoelectric materials a. Lithium niobate b. PZT c. PVDF

3.3. Acoustic Pressure Distribution

The acoustic pressure distribution was determined based on the resonance frequencies of each piezoelectric material. The result showed that the US transducer material has significant impact on the US waves magnitude and mode of propagation. The difference in the pattern of propagation of the US in the fluid media can be associated with the crystal orientation. The materials utilized have differences in their structure with PZT being perovskite, PVDF has orthorhombic, and Lithium niobate has trigonal crystal structure. This vast variation in their structures can be associated with the different patterns observed. In their study, Kuroiwa et al [29] highlighted that the large amount of the piezoelectric properties is attributed to their crystal orientation. As regards the magnitude of the US pressure, the increasing trend of the total acoustic pressure followed the order: PZT>Lithium niobate>PVDF under resonant conditions (Fig. 4). Although the PVDF has the least acoustic impedance (2.7×106 kg/m^{2}s), the acoustic pressure was lower than that of PZT. For example, whilst PVDF showed a maximum pressure of ~5.5×10^2Pa, PZT has a peak pressure of 3.5×10^5Pa. The possible reason for this is due to the high piezoelectric coefficient of 600 pC/N of PZT as compared to 33pC/N in the case of PVDF. The piezoelectric coefficient of Lithium niobate could reach 70 pC/N which makes them have an intermediate pressure between PZT and PVDF.
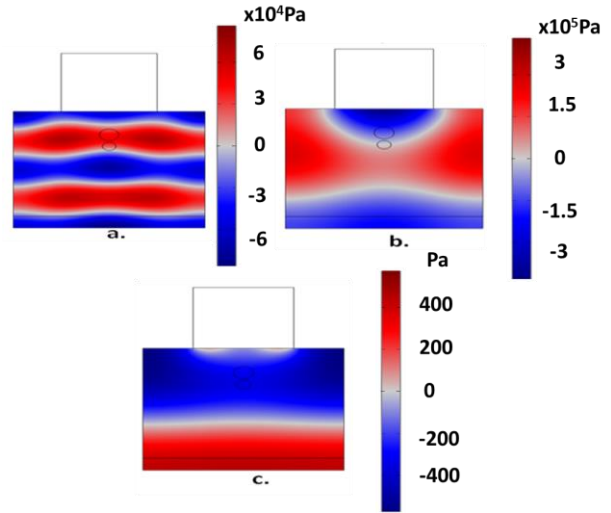
Fig. 4. Acoustic pressure distribution a. Lithium niobate b. PZT c. PVDF

3.4. Coalescence Time
3.4.1 Batch Conditions

The effect of the piezoelectric material type (PZT, PVDF and Lithium niobate) on the coalescence of two droplets of water in oil continuous phase was examined under batch conditions. The order of the coalescence time followed PZT< PVDF< Lithium niobate (Fig. 5). The coalescence times for PZT, PVDF and LiNbO$_3$ are 25.5, 27, and 92 ms, respectively. Likewise, the energy usage was 31.24, 33.08 and 112.7 mJ for PZT, PVDF and LiNbO3, respectively. This coalescence behavior is consistent with the determined acoustic pressure magnitudes, acoustic impedance and crystal orientation trend of the transducer materials. It is expected that as the acoustic pressure magnitude increases, the time taken for the coalescence of the droplets would reduce. The acoustic impedance and crystal orientation plays an important role as well with PVDF showing lower impedance as compared to PZT and LiNbO$_3$. Although the coalescence time of PZT is lower than that of PVDF and Lithium niobate, the overall assessment which includes environmental impact makes the lead free materials possible substitutes for PZT.
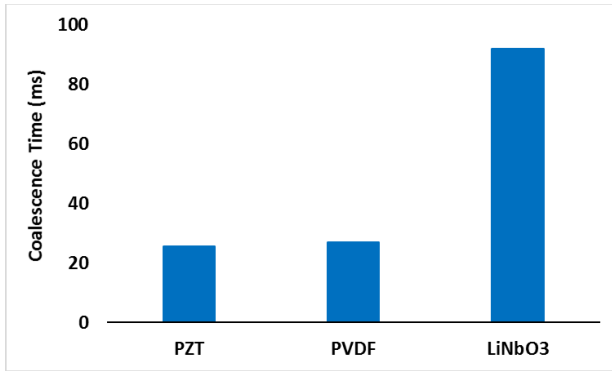
a.
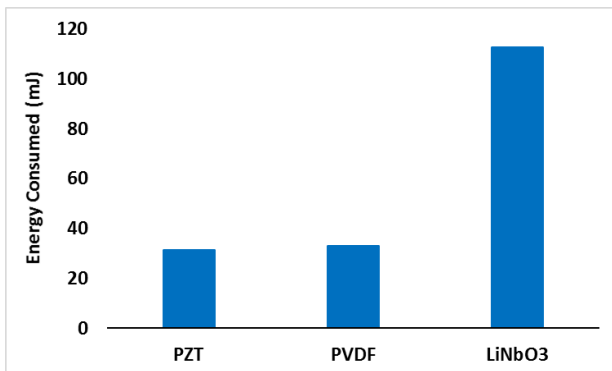
b.

Fig. 5. a. Coalescence time and **b.** energy consumption of the different piezoelectric materials utilized

3.4.2 Continuous Condition

The impact of flow velocity on the ultrasound coalescence of the water droplets in oil was assessed (Fig. 6). The coalescence time and energy consumption were evaluated at 100, 200 and 300 mm/s. Increasing velocities resulted in slight reduction in the coalescence time and energy consumed for the piezoelectric materials. For instance, the coalescence time with PZT decreased from 24.5ms to 22.5 ms as the flow velocity was increased from 100mm/s to 300mm/s. Likewise, the energy consumed was lowered from 30.01mJ to 27.56mJ within the same velocity range. The reduction in coalescence time and energy consumed with increasing flow velocity is beneficial for demulsification of crude oil during processing and transportation. Similar behavior of the coalescence dynamics of process time reduction was reported by Mardani et al [30]. The coalescence time followed an increasing order PZT<PVDF<LiNbO$_3$. At 100 mm/s, the coalescence times for PZT, PVDF and LiNbO$_3$ were 24.5, 28.5 and 87 ms, respectively. Moreover, PVDF showed non-coalescence at 300 mm/s, while LiNbO3 showed non-coalescence at 200 and 300 mm/s. PZT showed better coalescence performance of 1.16 and 3.55 times over PVDF and LiNbO$_3$, respectively. However, the significant benefits of utilizing lead free piezoelectric materials and other advantages of PVDF and LiNbO$_3$ make them attractive alternatives. The differences in the behavior of the piezoelectric transducer materials could be attributed to the variations in their piezoelectric coefficients, acoustic impedance and crystal orientations.
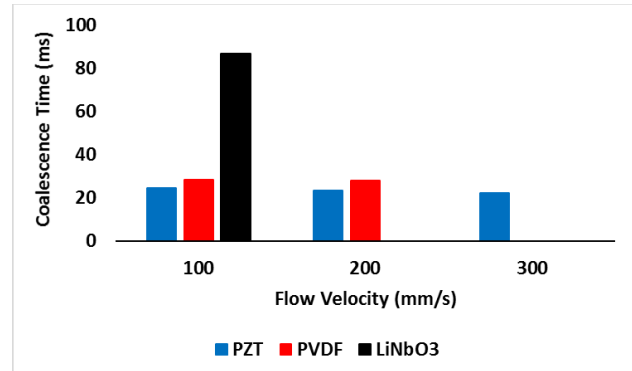
a.
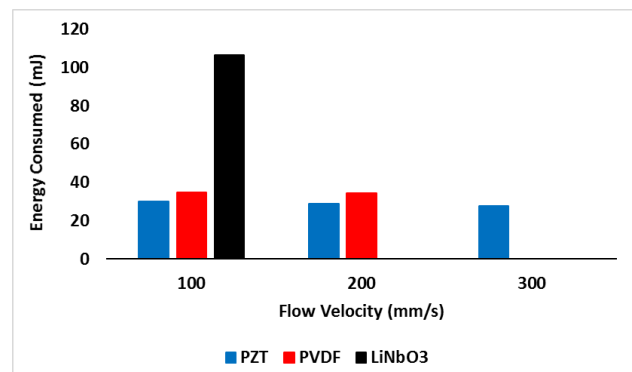
b.

Fig. 6. The effect of emulsion flow velocity on the **a.** coalescence time and **b.** energy consumed of different transducer materials

4. CONCLUSIONS

The assessment of the effect of different piezoelectric materials (PZT, PVDF and Lithium niobate) on the coalescence of two water droplets in oil was studied with a numerical model. The model predictions were validated with the experimental data of Luo et al [16] and showed reasonable agreement. The eigen-frequency analysis provided the resonance frequencies of 19.61, 26.04 and 57.80 kHz for PVDF, PZT and Lithium niobate, respectively. The acoustic pressure in the emulsion domain varied in magnitude and distribution. The variation in the acoustic pressure behavior could be attributed to the different crystal structure of the piezoelectric materials used. The order of the coalescence time for the binary droplets followed the order PZT <PVDF<Lithium niobate. The coalescence time for PZT was the lowest because of the higher acoustic pressure compared to the other materials. Even though the coalescence time of PZT is lower than that of PVDF and Lithium niobate, the potentiality of lead free piezoelectric materials becomes significant when the environmental and other advantages are considered. Moreover, increasing velocities resulted in slight reduction in the coalescence time and energy consumed for the piezoelectric materials. The reduction in coalescence time and energy consumed with increasing flow velocity is beneficial for demulsification of crude oil during processing and transportation.

Acknowledgements

References

[1] Koruza, J., Bell, A. J., Froemling, T., Webber, K. G., Wang, K., & Rödel, J. (2018). Requirements for the transfer of lead-free piezoceramics into application. Journal of Materiomics, 4(1), 13-26.

[2] Lemaire, E., Thuau, D., Souêtre, M., Zgainski, L., Royet, A., & Atli, A. (2021). Revisiting two piezoelectric salts within an eco-design paradigm for sensors and actuators applications. Sensors and Actuators A: Physical, 318, 112483.

[3] Rödel, J., Webber, K. G., Dittmer, R., Jo, W., Kimura, M., & Damjanovic, D. (2015). Transferring lead-free piezoelectric ceramics into application. Journal of the European Ceramic Society, 35(6), 1659-1681.

[4] Hussain, F., Khesro, A., Lu, Z., Wang, G., & Wang, D. (2020). Lead free multilayer piezoelectric actuators by economically new approach. Frontiers in Materials, 7, 87.

[5] Kosec, M., Malic, B., Wolny, W. W., James, A. S., Alemany, C., & Pardo, L. (1998). Effect of a chemically aggressive environment on the electromechanical behaviour of modified lead titanate ceramics. Journal-Korean Physical Society, 32, S1163-S1166.

[6] Ibn-Mohammed, T., Koh, S. C. L., Reaney, I. M., Sinclair, D. C., Mustapha, K. B., Acquaye, A., & Wang, D. (2017). Are lead-free piezoelectrics more environmentally friendly? MRS Communications, 7(1), 1-7.

[7] Regulation (EC) No 1907/2006 of the European Parliament and of the Council of 18 December 2006 concerning the Registration, Evaluation, Authorisation andRestriction ofChemicals(REACH), establishing a European Chemicals Agency, amending Directive 1999/45/EC and repealing Council Regulation (EEC) No 793/93 and Commission Regulation (EC) No 1488/94 as well as Council Directive 76/769/EEC and Commission Directives 91/155/EEC, 93/67/EEC, 93/105/EC and 2000/21/EC. Official Journal of the European Union 2006; L396:1–849.

[8] European Chemicals Agency. Inclusion ofsubstances of very high concern in the candidate list. vol. ED/169/2012; 2012.

[9] Xing, J., Jiang, L., Zhao, C., Tan, Z., Xu, Q., Wu, J., ... & Zhu, J. (2020). Potassium sodium niobate based lead-free ceramic for high-frequency ultrasound transducer applications. Journal of Materiomics, 6(3), 513-522.

[10] Wei, H., Wang, H., Xia, Y., Cui, D., Shi, Y., Dong, M., Liu, C., Ding, T., Zhang, J., Ma, Y. and Wang, N. (2018). An overview of lead-free piezoelectric materials and devices. Journal of Materials Chemistry C, 6(46), 12446-12467.

[11] Wu, J. (2018). Advances in lead-free piezoelectric materials (pp. 301-302). Singapore: Springer.

[12] Shibata, K., Wang, R., Tou, T., & Koruza, J. (2018). Applications of lead-free piezoelectric materials. Mrs Bulletin, 43(8), 612-616.

[13] Zheng, T., Wu, J., Xiao, D., & Zhu, J. (2018). Recent development in lead-free perovskite piezoelectric bulk materials. Progress in materials science, 98, 552-624.

[14] Zhang, S., & Yu, F. (2011). Piezoelectric materials for high temperature sensors. Journal of the American Ceramic Society, 94(10), 3153-3170.

[15] Vinogradov, A., & Holloway, F. (1999). Electro-mechanical properties of the piezoelectric polymer PVDF. Ferroelectrics, 226(1), 169-181.

[16] Luo, X., Cao, J., He, L., Wang, H., Yan, H., & Qin, Y. (2017). An experimental study on the coalescence process of binary droplets in oil under ultrasonic standing waves. Ultrasonics sonochemistry, 34, 839-846.

[17] Xu, Z. (2018). Numerical simulation of the coalescence of two bubbles in an ultrasound field. Ultrasonics sonochemistry, 49, 277-282.

[18] COMSOL Multi-physics. "CFD module user's guide 5.4." (2018).

[19] Osher, S., & Fedkiw, R. P. (2001). Level set methods: an overview and some recent results. Journal of Computational physics, 169(2), 463-502.

[20] Sethian, J. A. (1996). A fast marching level set method for monotonically advancing fronts. Proceedings of the National Academy of Sciences, 93(4), 1591-1595.

[21] Li, B., Vivacqua, V., Ghadiri, M., Sun, Z., Wang, Z., & Li, X. (2017). Droplet deformation under pulsatile electric fields. Chemical Engineering Research and Design, 127, 180-188.

[22] Vivacqua, V., Ghadiri, M., Abdullah, A. M., Hassanpour, A., Al-Marri, M. J., Azzopardi, B., Hewakandamby, B. & Kermani, B. (2016). Analysis of partial electrocoalescence by Level-Set and finite element methods. Chemical Engineering Research and Design, 114, 180-189.

[23] Lei, J., Cheng, F., & Li, K. (2020). Numerical Simulation of Boundary-Driven Acoustic Streaming in Microfluidic Channels with Circular Cross-Sections. Micromachines, 11(3), 240.

[24] Tsujino, J., Hongoh, M., Yoshikuni, M., Hashii, H., & Ueoka, T. (2004). Welding characteristics of 27, 40 and 67 kHz ultrasonic plastic welding systems using fundamental-and higher-resonance frequencies. Ultrasonics, 42(1-9), 131-137.

[25] Tsujino, J., Hongoh, M., Tanaka, R., Onoguchi, R., & Ueoka, T. (2002). Ultrasonic plastic welding using fundamental and higher resonance frequencies. Ultrasonics, 40(1-8), 375-378.

[26] Nakamura, S., Numasato, H., Sato, K., Kobayashi, M., & Naniwa, I. (2002). A push–pull multi-layered piggyback PZT actuator. Microsystem Technologies, 8(2-3), 149-154.

[27] Bawiec, C. R., Sunny, Y., Nguyen, A. T., Samuels, J. A., Weingarten, M. S., Zubkov, L. A., & Lewin, P. A. (2013). Finite element static displacement optimization of 20–100 kHz flexural transducers for

6

fully portable ultrasound applicator. Ultrasonics, 53(2), 511-517.

[28] Panda, P. K., & Sahoo, B. (2015). PZT to lead free piezo ceramics: a review. Ferroelectrics, 474(1), 128-143.

[29] Kuroiwa, Y., Kim, S., Fujii, I., Ueno, S., Nakahira, Y., Moriyoshi, C., Sato, Y. and Wada, S., 2020. Piezoelectricity in perovskite-type pseudo-cubic ferroelectrics by partial ordering of off-centered cations. Nature Communications Materials, 1.

[30] Mardani, M. R., Ganji, D. D., & Hosseinzadeh, K. (2022). Numerical investigation of droplet coalescence of saltwater in the crude oil by external electric field. Journal of Molecular Liquids, 346, 117111.